

MDPI

Article

A Nonlinear Control Design for Cooperative Adaptive Cruise Control with Time-Varying Communication Delay

Parisa Ansari Bonab *,† D and Arman Sargolzaei †

Department of Mechanical Engineering, University of South Florida, Tampa, FL 33620, USA; a.sargolzaei@gmail.com

- * Correspondence: parisaansaribonab@usf.edu
- [†] These authors contributed equally to this work.

Abstract: Cooperative adaptive cruise control (CACC) is one of the main features of connected and autonomous vehicles (CAVs), which uses connectivity to improve the efficiency of adaptive cruise control (ACC). The addition of reliable communication systems to ACC reduces fuel consumption, maximizes road capacity, and ensures traffic safety. However, the performance, stability, and safety of CACC could be affected by the transmission of outdated data caused by communication delays. This paper proposes a Lyapunov-based nonlinear controller to mitigate the impact of time-varying delays in the communication channel of CACC. This paper uses Lyapunov–Krasovskii functionals in the stability analysis to ensure semi-global uniformly ultimately bounded tracking. The efficaciousness of the proposed CACC algorithm is demonstrated in simulation and through experimental implementation.

Keywords: cooperative adaptive cruise control; time-varying delays; safe control design; Lyapunov–Krasovskii stability



Citation: Bonab, P.A.; Sargolzaei, A. A Nonlinear Control Design for Cooperative Adaptive Cruise Control with Time-Varying Communication Delay. *Electronics* **2024**, *13*, 1875. https://doi.org/10.3390/ electronics13101875

Academic Editor: Luca Patanè

Received: 23 February 2024 Revised: 23 April 2024 Accepted: 5 May 2024 Published: 10 May 2024



Copyright: © 2024 by the authors. Licensee MDPI, Basel, Switzerland. This article is an open access article distributed under the terms and conditions of the Creative Commons Attribution (CC BY) license (https://creativecommons.org/licenses/by/4.0/).

1. Introduction

Over the last decades, the automotive industry has demonstrated a growing interest in incorporating new technologies into vehicle design. These technologies, found in autonomous, connected, and electric vehicles, are primarily aimed at enhancing road safety and reducing the environmental impact of vehicular traffic [1,2].

Automated vehicles (AVs) and connected vehicles (CVs) provide complementary enhancements to transportation system performance and safety. Automation addresses challenges related to human driver limitations, while connectivity integrates vehicles and infrastructure, with the potential to improve environmental awareness, improve the safety of autonomous vehicles, overcome the constraints of perception systems, and enable an adaptable performance to achieve diverse goals. The integration of AVs and CVs as connected and autonomous vehicles (CAVs) has the potential to extend what driving automation and vehicle connectivity can achieve individually. In CAVs, autonomous vehicles can use connectivity, particularly Vehicle-to-Vehicle (V2V) and Vehicle-to-Infrastructure (V2I) communication. CAVs enable a variety of applications in intelligent transportation systems, including traffic control, cooperative driving, improved safety, and energy-efficient driving [3–5].

As part of AVs, adaptive cruise control (ACC) systems have been developed to keep a safe following distance between vehicles in a platoon. The ACC system actively manages the longitudinal movement of the vehicle by analyzing data from onboard sensors regarding the vehicle's motion status and the surrounding environment. This functionality aims to alleviate driver fatigue and enhance vehicle safety [6]. The extension of ACC by exploiting V2V communication (which can be achieved with CAVs) results in cooperative adaptive cruise control (CACC), which is a fundamental aspect of CAVs. Since CACC utilizes the

onboard sensors of ACC and wireless communication with other vehicles, it has access to enhanced information so that each vehicle can follow its predecessor with higher accuracy, faster response, and shorter gaps to enhance traffic flow stability and possibly improve safety [7–9].

CACC and other multi-agent systems rely heavily on the timely and accurate transmission of data between vehicles; as a result, they could be unreliable because of failures resulting from communication-related constraints [10–13]. To guarantee the safety of CACC, any possible time delays in the communication channel should be considered. To clarify, if data transmitted from the leader to the follower vehicle are delayed, then it affects the performance, stability, and safety of CACC, and results in collision.

The design and implementation of CACC has been considered in the literature. In [14], CACC was designed and implemented in real-world settings. This study also analyzed the string stability of the vehicles. Another study [15] presents the design, development, implementation, and testing of a CACC system. It consists of two controllers, one to manage the approaching maneuver to the leading vehicle and the other to regulate car-following once the vehicle joins the platoon. Both studies have addressed the issue of communication channel delays stemming from factors such as queueing, contention, transmission, and propagation. However, they have only accounted for a constant time delay.

In addition, the development of CACC under time delay in the communication channel is investigated in [16]. In this study, a CACC algorithm was developed while considering constant time delay in the communication channel. In another relevant study, a novel CACC algorithm using observer-based sliding mode control was developed [17]. This method effectively estimates uncertainties in both actuator and preceding vehicle acceleration, treating them as lumped disturbances. By doing so, the proposed strategy tackles real-world challenges like the unavailability of preceding vehicle acceleration data and the variability in vehicle dynamics. This paper also considered a constant delay in the communication channel. The authors of [18] investigated CACC under constant time delay in a communication channel by introducing an innovative method for designing an AV controller using modern machine learning techniques. Specifically, it demonstrates the application of reinforcement learning to develop controllers for the safe longitudinal following of a lead vehicle. However, all the above-mentioned papers have considered constant time delay in the communication channel but the communication delay is timevarying in real-world situations, which is more challenging. Additionally, their control algorithms designed for CACC are not obtained from well-established Lyapunov-based stability analyses. Furthermore, the current CACC approaches are unable to alleviate the effects of external disturbance and measurement noise in the presence of time-varying time-delays in communication channels.

Unlike other studies in the literature with constant communication delay, this paper has considered time-varying time delay in the communication channel of CACC. In addition, external disturbance and measurement noise have been considered. To address these challenges, a Lyapunov-based nonlinear controller is designed to mitigate the communication time delay, measurement noise, and disturbance effects in real-time. The Lyapunov-based stability of the proposed controller has been investigated in this paper using Lyapunov-Krasovskii (LK) functionals, which ensures that vehicles follow each other with a minimum safe distance. The effectiveness of the proposed safe controller is shown in both simulation and experimental environments.

The outline of the paper is as follows: Section 2 describes the mathematical model of CACC. The problem statement is explained in Section 3. Section 4 overviews the developed control design. The stability analysis of the designed controller is explained in Section 5. Section 6 presents the results and, finally, Section 7 discusses the conclusion and future work.

2. Mathematical Model of CACC

A CACC-equipped string of vehicles with time-varying delay in the communication channel is demonstrated in Figure 1. It is assumed that the control command of the lead vehicle is transmitted to the following vehicle through a communication channel. Also, the velocity and position of the lead vehicle are estimated by radar sensor. This paper assumed a platoon of vehicles with identical dynamic models for all vehicles for simplicity. The dynamic model of the vehicles is derived from real-world testing and detailed in Section 6. The dynamic model of *i*th vehicle is defined as

$$\begin{cases} \dot{x}_{i}(t) = v_{i}(t), \\ \dot{v}_{i}(t) = -\eta_{i}v_{i}(t) + \rho_{i}u_{i}(t) + d_{i}(t) + \theta_{i}(t), \end{cases}$$
(1)

where $i \in \{2, \dots, n\}$ denotes the follower vehicle, n is the number of vehicles, and i-1 indicates the lead vehicle. Each vehicle follows its own leader, and equations are for follower i with the leader i-1. In Equation (1), $x_i \in \mathbb{R}$, $v_i \in \mathbb{R}$, $u_i \in \mathbb{R}$, $d_i \in \mathbb{R}$, and $\theta_i \in \mathbb{R}$ represent the position, velocity, control input, external disturbance, and measurement noise, respectively. Also, η_i and ρ_i are constant parameters. Similarly, the dynamic model of the lead vehicle is defined as

$$\begin{cases} \dot{x}_{i-1}(t) = v_{i-1}(t), \\ \dot{v}_{i-1}(t) = -\eta_{i-1}v_{i-1}(t) + \rho_{i-1}u_{i-1}(t) + d_{i-1}(t) + \theta_{i-1}(t), \end{cases}$$
 (2)

where $x_{i-1} \in \mathbb{R}$, $v_{i-1} \in \mathbb{R}$, $u_{i-1} \in \mathbb{R}$, $d_{i-1} \in \mathbb{R}$, and $\theta_{i-1} \in \mathbb{R}$ represent the position, velocity, control input, external disturbance, and measurement noise, respectively. Since vehicles are homogeneous, $\eta_{i-1} = \eta_i$ and $\rho_{i-1} = \rho_i$.

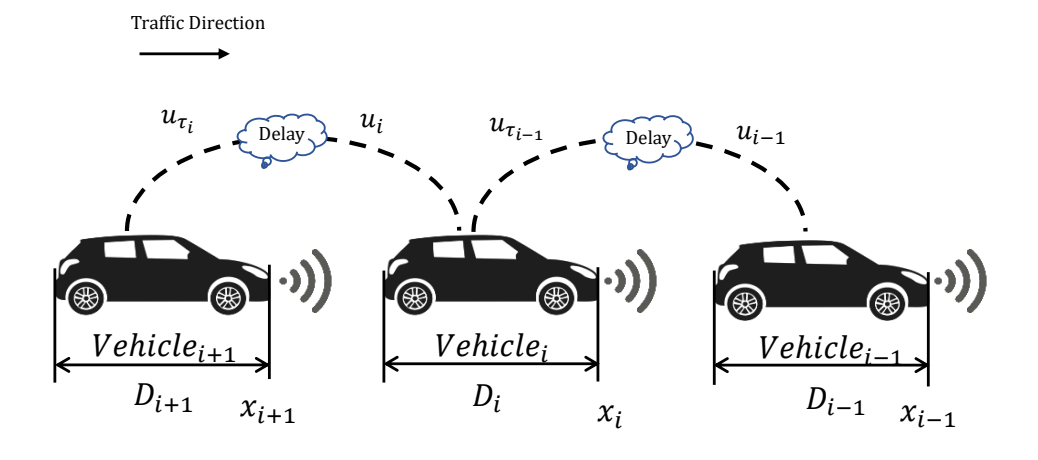


Figure 1. CACC-equipped string of vehicles with the communication time delay.

Assumption 1. The disturbances are assumed to be continuous and bounded by known constants such that $||d_i(t)|| < \bar{d}_{1_i}$ and $||d_{i-1}(t)|| < \bar{d}_{2_i}$ for $t \ge t_0$, and \bar{d}_{1_i} , $\bar{d}_{2_i} \in \mathbb{R}_{>0}$ [19].

Assumption 2. The noises are bounded Gaussian measurement noises such that $\|\theta_i(t)\| < \bar{\theta}_{1_i}$ and $\|\theta_{i-1}(t)\| < \bar{\theta}_{2_i}$ for $t \ge t_0$, and $\bar{\theta}_{1_i}$, $\bar{\theta}_{2_i} \in \mathbb{R}_{>0}$ [19].

Electronics **2024**, 13, 1875 4 of 16

Communication Channel with Time Delay

It is assumed that the lead vehicle's control signal is transmitted to the follower vehicle with a time-varying delay. As a result, the follower vehicle relies on outdated data. The lead vehicle transmits $u_{i-1}(t)$ to its follower; however, it receives $u_{\tau_{i-1}}(t)$, which is defined as

$$u_{\tau_{i-1}}(t) \triangleq u_{i-1}(t - \tau_i(t)),\tag{3}$$

where $\tau_i(t) \in \mathbb{R}$ represents a known positive time-varying signal.

Assumption 3. The time-varying delay is bounded and differentiable such that $0 < \tau_i(t) \le \bar{\tau}_i$, $\forall t \in \mathbb{R}_{>0}$, where $\bar{\tau}_i$ is a positive known constant. The rate of change for the delay is bounded such that $|\dot{\tau}_i(t)| < \dot{\tau}_{Max} < 1$, $\forall t \in \mathbb{R}_{>0}$, where $\dot{\tau}_{Max}$ is a positive known constant [20].

Assumption 4. The leader's control signal is assumed to be bounded by a known constant such that $\|u_{i-1}(t)\| \le \bar{u}_{i-1}$, where \bar{u}_{i-1} is a positive known constant. Then, we can conclude that $u_{\tau_{i-1}}$ is also bounded such that $\|u_{\tau_{i-1}}\| \le \bar{u}_{\tau_{i-1}}$, where $\bar{u}_{\tau_{i-1}}$ is a positive known constant (due to physical constraints, the control signal of the lead vehicle is bounded).

3. Problem Statement

The main objective of this paper is to design a safe controller for CACC, addressing the impact of time delay on vehicles' communication channels. The aim is to ensure a safe following distance between the leader and follower vehicles. In the CACC algorithm, a real-time control signal from the lead vehicle is transmitted to the follower vehicle. However, the time delay within the communication channel causes the transmission of the outdated control signal to the follower. One challenge here is that the u_i uses delayed u_{i-1} , which poses a potential risk of collisions. Therefore, to obtain a delay-free control signal of the leader, we developed a predictor term $e_{u_{i-1}} \in \mathbb{R}$ as

$$e_{u_{i-1}}(t) \triangleq \int_{t-\tau_i(t)}^t u_{i-1}(s) \, ds,\tag{4}$$

the time derivative of (4) is calculated as

$$\dot{e}_{u_{i-1}}(t) = u_{i-1}(t) - (1 - \dot{\tau}_i(t))u_{\tau_{i-1}}(t),\tag{5}$$

for simplification, we define $\phi_i(t) \triangleq 1 - \dot{\tau}_i(t)$.

Remark 1. Considering Assumption 3, $\phi_i(t)$ is also bounded such that $\|\phi_i(t)\| < \bar{\phi}_i$, where $\bar{\phi}_i$ is a known positive constant.

Besides defining $e_{u_{i-1}}(t)$ in (4), to measure the objective, we introduce other error signals, including a distance error and an auxiliary error to facilitate the stability analysis. The distance error $e_i : [t_0, \infty) \to \mathbb{R}$ is defined as

$$e_i(t) \triangleq x_i(t) - x_{i-1}(t) + D_i + x_{d_i}(t),$$
 (6)

where $D_i \in \mathbb{R}$ is the length of vehicle and $x_{d_i} \in \mathbb{R}$ is the desired distance between vehicles, and auxiliary error $r_i \in \mathbb{R}$ is defined as

$$r_i(t) \stackrel{\Delta}{=} \dot{e}_i(t) + \lambda_i e_i(t) + \rho_i e_{u_{i-1}}(t), \tag{7}$$

where $\lambda_i \in \mathbb{R}_{>0}$, is a user-defined gain.

Assumption 5. The desired distance and its first and second derivatives are assumed to be bounded by positive known constants, x_{d_i} , \dot{x}_{d_i} , \dot{x}_{d_i} , $\dot{x}_{d_i} \in \mathcal{L}_{\infty}$ [21].

4. Proposed Control Design

In order to address the problem statement, we develop a nonlinear Lyapunov-based controller. The control signal is designed using the Lyapunov stability analysis in Section 5 as.

$$u_{i}(t) \triangleq \frac{\eta_{i}}{\rho_{i}} v_{i}(t) - \frac{\eta_{i-1}}{\rho_{i-1}} v_{i-1}(t) - \frac{1}{\rho_{i}} \ddot{x}_{d_{i}}(t) - \frac{\lambda_{i}}{\rho_{i}} r_{i}(t) + \phi_{i}(t) u_{\tau_{i-1}}(t) + \frac{\lambda_{i}^{2}}{\rho_{i}} e_{i}(t) + \lambda_{i} e_{u_{i-1}}(t) - \frac{K_{i}}{\rho_{i}} r_{i}(t) - \frac{1}{\rho_{i}} e_{i}(t),$$
(8)

where $K_i \in \mathbb{R}$ is a positive user-defined gain.

The closed-loop form of the system can be calculated as the time derivative of $r_i(t)$ as

$$\dot{r}_i(t) = \ddot{e}_i(t) + \lambda_i \dot{e}_i(t) + \rho_i \dot{e}_{u_{i-1}}(t). \tag{9}$$

Substituting the second time derivative of (6) and $\dot{e}_i(t)$ from (7) in (9) yields

$$\dot{r}_{i}(t) = \ddot{x}_{i}(t) - \ddot{x}_{i-1}(t) + \ddot{x}_{d_{i}}(t) + \lambda_{i}r_{i}(t) - \lambda_{i}^{2}e_{i}(t)
- \lambda_{i}\rho_{i}e_{u_{i-1}}(t) + \rho_{i}\dot{e}_{u_{i-1}}(t).$$
(10)

Using the dynamic model of vehicles in (1), (2), and (5) results in

$$\dot{r}_{i}(t) = -\eta_{i}v_{i}(t) + \rho_{i}u_{i}(t) + d_{i}(t) + \theta_{i}(t) + \eta_{i-1}v_{i-1}(t)
- \rho_{i-1}u_{i-1}(t) - d_{i-1}(t) - \theta_{i-1}(t) + \ddot{x}_{d_{i}}(t)
+ \lambda_{i}r_{i}(t) - \lambda_{i}^{2}e_{i}(t) - \lambda_{i}\rho_{i}e_{u_{i-1}}(t) + \rho_{i}u_{i-1}(t)
- \rho_{i}\phi_{i}(t)u_{\tau_{i-1}}(t).$$
(11)

Further simplification and substituting $u_i(t)$ from (8) into (11) results

$$\dot{r}_i(t) = -K_i r_i(t) - e_i(t) + d_i(t) - d_{i-1}(t)
+ \theta_i(t) - \theta_{i-1}(t).$$
(12)

By defining an auxiliary term of $N_i(t) \triangleq d_i(t) - d_{i-1}(t) + \theta_i(t) - \theta_{i-1}(t)$, (12) changes to

$$\dot{r}_i(t) = -K_i r_i(t) - e_i(t) + N_i(t). \tag{13}$$

Remark 2. Assumptions 1 and 2 are used to show that N_i is bounded such that $||N_i|| \leq \bar{N}_i$, where $\bar{N}_i \in \mathbb{R}_{>0}$.

In the next section, the sign t, representing time, is dropped for the simplicity of the equations.

5. Stability Analysis

To facilitate the stability analysis, let the stacked error be denoted by $z_i \in \mathbb{R}^2$, which is defined as

$$z_i \triangleq [e_i^T, r_i^T]^T. \tag{14}$$

Moreover, let $\Xi_i \in \mathbb{R}^4$ be defined as

$$\Xi_i \triangleq [z_i^T, \sqrt{P_{LK_i}}, \sqrt{Q_{LK_i}}]^T, \tag{15}$$

where P_{LK_i} and Q_{LK_i} : $[t_0, \infty) \to \mathbb{R}_{\geq 0}$ are LK functionals, which are defined as

$$P_{LK_i} \triangleq \omega_{1_i} \int_{t-\tau_i}^{t} ||u_{i-1}(s)||^2 ds,$$
 (16)

$$Q_{LK_i} \triangleq \omega_{2_i} \int_{t-\tau_i}^t \left(\int_{\theta}^t \|u_{i-1}(s)\|^2 ds \right) d\theta, \tag{17}$$

where $\omega_{1_i}, \omega_{2_i} \in \mathbb{R}_{\geq 0}$ are user-defined constants.

Applying the Leibniz derivative rule to (16) and (17) results in

$$\dot{P}_{LK_i} = \omega_{1,i} \|u_{i-1}\|^2 - \omega_{1,i} \phi_i \|u_{\tau_{i-1}}\|^2, \tag{18}$$

$$\dot{Q}_{LK_i} = \omega_{2_i} \tau_i \|u_{i-1}\|^2 - \omega_{2_i} \phi_i \int_{t-\tau_i}^t \|u_{i-1}\|^2 ds.$$
 (19)

Let the following be the sufficient conditions

$$\lambda_{i} > \frac{\rho_{i}}{2\varepsilon_{1_{i}}},$$

$$K_{i} > \frac{1}{2\varepsilon_{2_{i}}},$$

$$\omega_{2_{i}} > \frac{\rho_{i}\varepsilon_{1_{i}}\tau_{i}}{\phi_{i}},$$
(20)

where ε_{1_i} , $\varepsilon_{2_i} \in \mathbb{R}_{>0}$ denote positive known constants. Also, ω_{1_i} should be selected as a small positive value.

Based on the sufficient conditions presented in (20), we define the positive variables α_{p_i} for $p \in \{1,2,3\}$ as

$$\alpha_{1_{i}} \stackrel{\Delta}{=} \lambda_{i} - \frac{\rho_{i}}{2\varepsilon_{1_{i}}},$$

$$\alpha_{2_{i}} \stackrel{\Delta}{=} K_{i} - \frac{1}{2\varepsilon_{2_{i}}},$$

$$\alpha_{3_{i}} \stackrel{\Delta}{=} \frac{\omega_{2_{i}}\phi_{i}}{2\tau_{i}} - \frac{\rho_{i}\varepsilon_{1_{i}}}{2}.$$
(21)

Furthermore, let $\beta_{1_i} \stackrel{\Delta}{=} \min\{\alpha_{1_i}, \alpha_{2_i}\}$, and $\beta_{2_i} \stackrel{\Delta}{=} \min\{\beta_{1_i}, \frac{\omega_{2_i}\phi_i}{4\omega_{1_i}}, \frac{\phi_i}{4\bar{\tau}_i}\}$.

Also, φ_i is defined as

$$\varphi_i \stackrel{\Delta}{=} \frac{\varepsilon_{2_i}}{2} \bar{N}_i^2 + (\omega_{1_i} + \omega_{2_i} \bar{\tau}_i) \bar{u}_{i-1}^2 + \omega_{1_i} \bar{\phi}_i \bar{u}_{\tau_{i-1}}^2.$$
 (22)

Theorem 1. For the dynamics in (1) and (2), the controller designed in (8) ensures semi-globally uniformly ultimately bounded tracking such that

$$\limsup_{t \to \infty} \|\Xi_i(t)\| \le \sqrt{2\frac{\varphi_i}{\beta_{2_i}}},\tag{23}$$

given that Assumptions 1–5 are satisfied and the sufficient conditions in (20) are satisfied.

Proof. Let $V_i : \mathbb{R}^4 \times [0, \infty) \to \mathbb{R}_{\geq 0}$ denote a radially unbounded, positive definite, continuously differentiable Lyapunov function defined as

$$V_i \triangleq \frac{1}{2}e_i^2 + \frac{1}{2}r_i^2 + P_{LK_i} + Q_{LK_i}, \tag{24}$$

which is bounded such that it holds the following inequality

$$\frac{1}{2}\|\Xi_i\|^2 \le V_i \le \|\Xi_i\|^2. \tag{25}$$

Taking the derivative of (24) yields

$$\dot{V}_{i} = e_{i}\dot{e}_{i} + r_{i}\dot{r}_{i} + \dot{P}_{LK_{i}} + \dot{Q}_{LK_{i}}, \tag{26}$$

substituting \dot{e}_i from (7) and (13) into (26) yields

$$\dot{V}_i = e_i(r_i - \lambda_i e_i - \rho_i e_{u_{i-1}}) + r_i(-K_i r_i - e_i + N_i) + \dot{P}_{I,K_i} + \dot{Q}_{I,K_i},$$
(27)

simplification results in

$$\dot{V}_{i} = -\lambda_{i}e_{i}^{2} - \rho_{i}e_{i}e_{u_{i-1}} - K_{i}r_{i}^{2} + r_{i}N_{i}
+ \dot{P}_{LK_{i}} + \dot{Q}_{LK_{i'}}$$
(28)

substituting from (18) and (19) into (28) results in

$$\dot{V}_{i} = -\lambda_{i}e_{i}^{2} - \rho_{i}e_{i}e_{u_{i-1}} - K_{i}r_{i}^{2} + r_{i}N_{i}
+ \omega_{1_{i}}\|u_{i-1}\|^{2} - \omega_{1_{i}}\phi_{i}\|u_{\tau_{i-1}}\|^{2}
+ \omega_{2_{i}}\tau_{i}\|u_{i-1}\|^{2} - \omega_{2_{i}}\phi_{i}\int_{t-\tau_{i}}^{t}\|u_{i-1}\|^{2}ds.$$
(29)

Young's Inequality can be applied to select terms in (29) as

$$e_{i}e_{u_{i-1}} \leq \frac{1}{2\varepsilon_{1_{i}}} \|e_{i}\|^{2} + \frac{\varepsilon_{1_{i}}}{2} \|e_{u_{i-1}}\|^{2},$$

$$r_{i}N_{i} \leq \frac{1}{2\varepsilon_{2_{i}}} \|r_{i}\|^{2} + \frac{\varepsilon_{2_{i}}}{2} \|N_{i}\|^{2},$$
(30)

by applying Young's Inequality in (29), the following inequality is obtained:

$$\dot{V}_{i} \leq -\lambda_{i} \|e_{i}\|^{2} + \frac{\rho_{i}}{2\varepsilon_{1_{i}}} \|e_{i}\|^{2} + \frac{\rho_{i}\varepsilon_{1_{i}}}{2} \|e_{u_{i-1}}\|^{2}
-K_{i} \|r_{i}\|^{2} + \frac{1}{2\varepsilon_{2_{i}}} \|r_{i}\|^{2} + \frac{\varepsilon_{2_{i}}}{2} \|N_{i}\|^{2}
+\omega_{1_{i}} \|u_{i-1}\|^{2} + \omega_{1_{i}} \bar{\phi}_{i} \|u_{\tau_{i-1}}\|^{2}
+\omega_{2_{i}} \bar{\tau}_{i} \|u_{i-1}\|^{2} - \omega_{2_{i}} \phi_{i} \int_{t-\tau}^{t} \|u_{i-1}\|^{2} ds,$$
(31)

using Cauchy–Schwarz inequality [22], the integral term in (31) can be replaced with an upper bound as

$$\dot{V}_{i} \leq -\lambda_{i} \|e_{i}\|^{2} + \frac{\rho_{i}}{2\varepsilon_{1_{i}}} \|e_{i}\|^{2} + \frac{\rho_{i}\varepsilon_{1_{i}}}{2} \|e_{u_{i-1}}\|^{2}
-K_{i} \|r_{i}\|^{2} + \frac{1}{2\varepsilon_{2_{i}}} \|r_{i}\|^{2} + \frac{\varepsilon_{2_{i}}}{2} \|N_{i}\|^{2}
+ \omega_{1_{i}} \|u_{i-1}\|^{2} + \omega_{1_{i}}\bar{\phi}_{i} \|u_{\tau_{i-1}}\|^{2} + \omega_{2_{i}}\bar{\tau}_{i} \|u_{i-1}\|^{2}
- \frac{\omega_{2_{i}}\phi_{i}}{2\tau_{i}} \|e_{u_{i-1}}\|^{2} - \frac{\omega_{2_{i}}\phi_{i}}{2} \int_{t-\tau_{i}}^{t} \|u_{i-1}\|^{2} ds.$$
(32)

Applying Cauchy–Schwarz inequality again, the integral term in (32) can be replaced with an upper bound as

$$\dot{V}_{i} \leq -\lambda_{i} \|e_{i}\|^{2} + \frac{\rho_{i}}{2\varepsilon_{1_{i}}} \|e_{i}\|^{2} + \frac{\rho_{i}\varepsilon_{1_{i}}}{2} \|e_{u_{i-1}}\|^{2}
-K_{i} \|r_{i}\|^{2} + \frac{1}{2\varepsilon_{2_{i}}} \|r_{i}\|^{2} + \frac{\varepsilon_{2_{i}}}{2} \|N_{i}\|^{2}
+\omega_{1_{i}} \|u_{i-1}\|^{2} + \omega_{1_{i}}\bar{\phi}_{i} \|u_{\tau_{i-1}}\|^{2} + \omega_{2_{i}}\bar{\tau}_{i} \|u_{i-1}\|^{2}
-\frac{\omega_{2_{i}}\phi_{i}}{2\tau_{i}} \|e_{u_{i-1}}\|^{2} - \frac{\omega_{2_{i}}\phi_{i}}{4} \int_{t-\tau_{i}}^{t} \|u_{i-1}\|^{2} ds
-\frac{\omega_{2_{i}}\phi_{i}}{4\bar{\tau}_{i}} \left(\int_{t-\tau_{i}}^{t} \left(\int_{\theta}^{t} \|u_{i-1}\|^{2} ds\right) d\theta\right);$$
(33)

combining similar terms results in

$$\dot{V}_{i} \leq \left(-\lambda_{i} + \frac{\rho_{i}}{2\varepsilon_{1_{i}}}\right) \|e_{i}\|^{2} + \left(-\frac{\omega_{2_{i}}\phi_{i}}{2\tau_{i}} + \frac{\rho_{i}\varepsilon_{1_{i}}}{2}\right) \|e_{u_{i-1}}\|^{2} \\
+ \left(-K_{i} + \frac{1}{2\varepsilon_{2_{i}}}\right) \|r_{i}\|^{2} + \frac{\varepsilon_{2_{i}}}{2} \|N_{i}\|^{2} \\
+ \left(\omega_{1_{i}} + \omega_{2_{i}}\bar{\tau}_{i}\right) \|u_{i-1}\|^{2} + \omega_{1_{i}}\bar{\phi}_{i} \|u_{\tau_{i-1}}\|^{2} \\
- \frac{\omega_{2_{i}}\phi_{i}}{4} \int_{t-\tau_{i}}^{t} \|u_{i-1}\|^{2} ds \\
- \frac{\omega_{2_{i}}\phi_{i}}{4\bar{\tau}_{i}} \left(\int_{t-\tau_{i}}^{t} \left(\int_{\theta}^{t} \|u_{i-1}\|^{2} ds\right) d\theta\right).$$
(34)

Substituting from (16) and (17) changes (34) to

$$\dot{V}_{i} \leq \left(-\lambda_{i} + \frac{\rho_{i}}{2\varepsilon_{1_{i}}}\right) \|e_{i}\|^{2} + \left(-\frac{\omega_{2_{i}}\phi_{i}}{2\tau_{i}} + \frac{\rho_{i}\varepsilon_{1_{i}}}{2}\right) \|e_{u_{i-1}}\|^{2} \\
+ \left(-K_{i} + \frac{1}{2\varepsilon_{2_{i}}}\right) \|r_{i}\|^{2} + \frac{\varepsilon_{2_{i}}}{2} \|N_{i}\|^{2} \\
+ \left(\omega_{1_{i}} + \omega_{2_{i}}\bar{\tau}_{i}\right) \|u_{i-1}\|^{2} + \omega_{1_{i}}\bar{\phi}_{i} \|u_{\tau_{i-1}}\|^{2} \\
- \frac{\omega_{2_{i}}\phi_{i}}{4\omega_{1_{i}}} P_{LK_{i}} - \frac{\phi_{i}}{4\bar{\tau}_{i}} Q_{LK_{i}}, \tag{35}$$

considering Assumption 4 and using $||N_i|| \leq \bar{N}_i$, the following inequality can be obtained:

$$\dot{V}_{i} \leq \left(-\lambda_{i} + \frac{\rho_{i}}{2\varepsilon_{1_{i}}}\right) \|e_{i}\|^{2} + \left(-\frac{\omega_{2_{i}}\phi_{i}}{2\tau_{i}} + \frac{\rho_{i}\varepsilon_{1_{i}}}{2}\right) \|e_{u_{i-1}}\|^{2} \\
+ \left(-K_{i} + \frac{1}{2\varepsilon_{2_{i}}}\right) \|r_{i}\|^{2} + \frac{\varepsilon_{2_{i}}}{2} \bar{N}_{i}^{2} \\
+ \left(\omega_{1_{i}} + \omega_{2_{i}}\bar{\tau}_{i}\right) \bar{u}_{i-1}^{2} + \omega_{1_{i}}\bar{\phi}_{i}\bar{u}_{\tau_{i-1}}^{2} \\
- \frac{\omega_{2_{i}}\phi_{i}}{4\omega_{1_{i}}} P_{LK_{i}} - \frac{\phi_{i}}{4\bar{\tau}_{i}} Q_{LK_{i}}, \tag{36}$$

applying (22) changes (36) to

$$\dot{V}_{i} \leq \left(-\lambda_{i} + \frac{\rho_{i}}{2\varepsilon_{1_{i}}}\right) \|e_{i}\|^{2} + \left(-\frac{\omega_{2_{i}}\phi_{i}}{2\tau_{i}} + \frac{\rho_{i}\varepsilon_{1_{i}}}{2}\right) \|e_{u_{i-1}}\|^{2}
+ \left(-K_{i} + \frac{1}{2\varepsilon_{2_{i}}}\right) \|r_{i}\|^{2} - \frac{\omega_{2_{i}}\phi_{i}}{4\omega_{1_{i}}} P_{LK_{i}}
- \frac{\phi_{i}}{4\bar{\tau}_{i}} Q_{LK_{i}} + \varphi_{i},$$
(37)

substituting the variables defined in (21) in (37) changes it to

$$\dot{V}_{i} \leq -\alpha_{1_{i}} \|e_{i}\|^{2} - \alpha_{2_{i}} \|r_{i}\|^{2} - \alpha_{3_{i}} \|e_{u_{i-1}}\|^{2}
- \frac{\omega_{2_{i}} \phi_{i}}{4\omega_{1_{i}}} P_{LK_{i}} - \frac{\phi_{i}}{4\bar{\tau}_{i}} Q_{LK_{i}} + \varphi_{i},$$
(38)

since $\beta_{1_i} \stackrel{\Delta}{=} \min\{\alpha_{1_i}, \alpha_{2_i}\}$, and using (14), the following is obtained from (38):

$$\dot{V}_{i} \leq -\beta_{1_{i}} \|z_{i}\|^{2} - \alpha_{3_{i}} \|e_{u_{i-1}}\|^{2}
- \frac{\omega_{2_{i}} \phi_{i}}{4\omega_{1_{i}}} P_{LK_{i}} - \frac{\phi_{i}}{4\overline{\tau}_{i}} Q_{LK_{i}} + \varphi_{i}.$$
(39)

In (39), the term $-\alpha_{3_i} \|e_{u_{i-1}}\|^2$ is a negative value, from this the following can be concluded:

$$\dot{V}_{i} \leq -\beta_{1_{i}} \|z_{i}\|^{2} - \frac{\omega_{2_{i}} \phi_{i}}{4\omega_{1_{i}}} P_{LK_{i}} - \frac{\phi_{i}}{4\bar{\tau}_{i}} Q_{LK_{i}} + \varphi_{i}, \tag{40}$$

using $\beta_{2_i} \stackrel{\Delta}{=} \min\{\beta_{1_i}, \frac{\omega_{2_i}\phi_i}{4\omega_{1_i}}, \frac{\phi_i}{4\bar{\tau}_i}\}$ and (15), (40) can be written as

$$\dot{V}_i \le -\beta_{2i} \|\Xi_i\|^2 + \varphi_i. \tag{41}$$

By substituting the upper bound for the Lyapunov function denoted in (25), (41) can be written as:

$$\dot{V}_i \le -\beta_{2_i} V_i + \varphi_i. \tag{42}$$

Solving (42) leads to (23), demonstrating that $\Xi_i(t)$ is bounded; therefore, from (15) it can be concluded that $z_i \in \mathcal{L}_{\infty}$, thus the semi-globally uniformly boundedness tracking is assured. \square

6. Results

This section presents and discusses the results of testing the proposed nonlinear controller using MATLAB R2023a Simulink and the experimental setup.

6.1. Vehicle Model through Experimental Analysis

The dynamic model of the vehicle, outlined in Section 2, was formulated based on experimental data obtained from a 2017 Ford Fusion Hybrid (depicted as the research vehicle in Figure 2). In this test scenario, the system's input is represented by the pedal percentage, with the measurable output being the vehicle velocity. Assuming the first-order transfer function of the *i*th vehicle is as

$$T_i(s) = \frac{V_i(s)}{U_i(s)},\tag{43}$$

where $T_i(s)$ is the first-order transfer function of the vehicle in the Laplace domain, s is the variable of Laplace domain, $V_i(s)$ is the Laplace form of the actual velocity, and $U_i(s)$ is the Laplace form of control command, which is the provided pedal percentage. In obtaining the transfer function of the vehicle, we conducted experimental tests with varied pedal percentage values. Subsequently, we determined the average actual velocity resulting from these tests. By computing the time constant (c_i) associated with the average output, we were able to ascertain the transfer function as

$$T_i(s) = \frac{\rho_i}{s+n_i},\tag{44}$$

where $\eta_i \in \mathbb{R}$ is a constant value obtained as below:

$$\eta_i \stackrel{\Delta}{=} \frac{1}{c_i},\tag{45}$$

and $\rho_i \in \mathbb{R}$ is obtained from below equation

$$\frac{\rho_i}{\eta_i} = \frac{v_{i_{\rm ss}}}{u_{i_{\rm cc}}},\tag{46}$$

where $v_{i_{ss}} \in \mathbb{R}$ is the steady state value of the actual velocity in the time domain, and $u_{i_{ss}} \in \mathbb{R}$ is the steady state value of the provided input. Using the Laplace inverse transform, the dynamic model of the ith vehicle is obtained from (43) and (44), which has been explained in Section 2. The values of parameters in (1), ρ_i and η_i , are presented in Table 1.



Figure 2. Experimental setup.

Table 1. Parameters.

Controller Gains	Disturbance	Communication Delay	Model Parameters
$\lambda_i = 1$	$d_i(t) = 0.01sin(t/4)$	$\tau_i(t) = \sigma \left(2\sin(t/2) + 3\right)$	$ \rho_i = 6.6870 $
$K_{1_i} = 0.5$	$d_{i-1}(t) = 0.01sin(t/4)$	σ is a coefficient that is varied.	$\eta_i = 0.1413$

6.2. Simulink Results

Here, we use MATLAB R2023a Simulink to validate the effectiveness of the developed controller.

As we discussed earlier, the aim of this study is to achieve two objectives simultaneously: maintaining a predefined distance between vehicles and tracking the speed of the lead vehicle. The desired distance is denoted as $x_{d_i} = 5m$. Also, we injected band-limited white noise in the Simulink as our measurement noise. Controller design parameters, disturbance, time delay signal, and vehicles' model parameters are added to Table 1.

In addition, Algorithm 1 illustrates the steps followed in this paper to design the controller.

The following figures show the effectiveness of the proposed approach. Figure 3 represents the distance between follower and lead vehicles under a communication time delay with $\sigma=0.02$, disturbance, and measurement noise. As shown in this figure, the proposed controller maintained the desired distance. However, there are some overshoots and undershoots in the figure; the controller is able to safely follow the lead vehicle. As shown in the figure, in the period of undershoot the distance between two vehicles is also safe. In the baseline controller, which is inspired by [2], where the controller lacks compensation for a time-varying time delay in the communication channel, numerous instances of overshooting and undershooting occur. This leads to vehicles being either closely packed or excessively spaced apart. In addition, our proposed controller does not lead to collision; however, the possibility of crash is high in the baseline controller.

Algorithm 1: Designed controller algorithm

Data: η_i , ρ_i , λ_i , K_i .

Begin

Initialize parameters

for t do

Compute the error signal from (4) to obtain a delay free control signal of the leader;

Compute the distance error signal from (6);

Compute the auxiliary error from (7);

Calculate the Control signal from (8);

The additional Figures 4–6, depicting the proposed controller and baseline controller with higher σ values, exhibit similar outcomes to Figure 3. The distinction lies in the fact that, as the magnitude of communication time delay increases, the baseline controller yields worse results, causing vehicles to either be excessively spaced apart or closely positioned. As illustrated in Figure 7 for $\sigma=0.1$, there are more oscillations in vehicle distance. In the undershoots, they move very close to each other, and there is a crash in their movement. However, the proposed controller outperformed the baseline controller, maintaining a safe distance between vehicles.

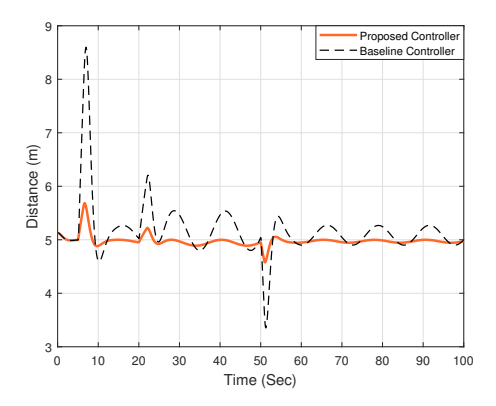


Figure 3. Distance between vehicles for $\sigma = 0.02$.

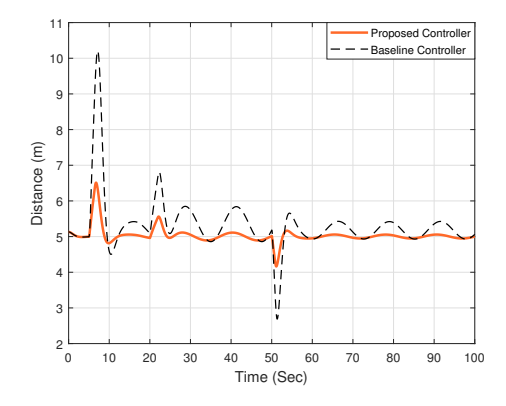


Figure 4. Distance between vehicles for $\sigma = 0.04$.

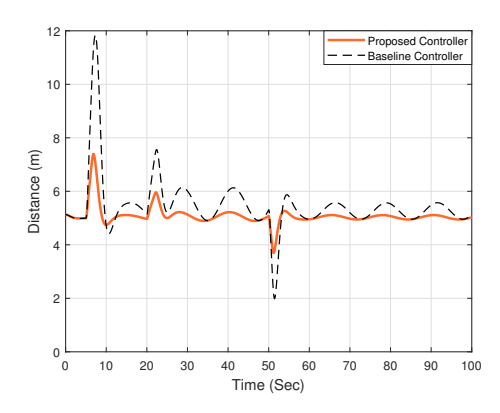


Figure 5. Distance between vehicles for $\sigma = 0.06$.

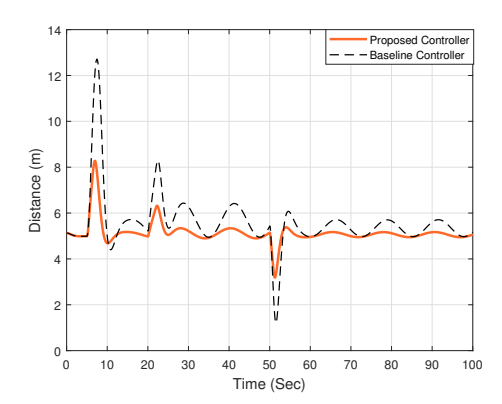


Figure 6. Distance between vehicles for $\sigma = 0.08$.

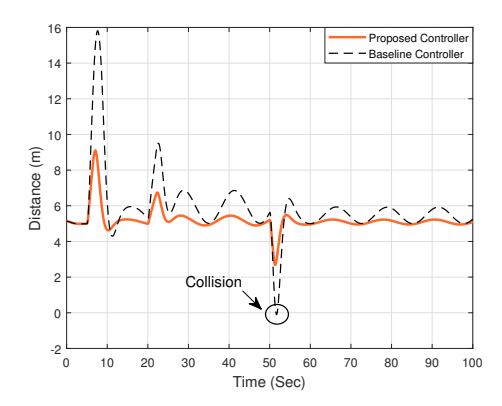


Figure 7. Distance between vehicles for $\sigma = 0.1$.

Table 2 shows how the proposed control algorithm mitigates the effects of the time delay in the communication channel. The first column of the table indicates σ , the second column indicates the Root Mean Square Error (RMSE) of the distance between vehicles and the desired distance using the proposed controller, and the last column of the table is the RMSE of the distance and the desired distance using the baseline controller. The RMSE data were collected for values of σ ranging from 0.02 to 0.1. These values were chosen to represent a range of operational conditions under which both controllers were evaluated.

The data indicate a consistent trend: as σ increases, the RMSE for both controllers increases. However, the rate of increase and the absolute values of RMSE are notably different between the two controllers. For σ values from 0.02 to 0.1, the proposed controller consistently exhibits a lower RMSE than the baseline controller. This suggests that the proposed controller is more accurate in these conditions. In contrast, the baseline controller shows a more significant increase in RMSE, especially beyond $\sigma=0.06$. This sharp

increase—particularly between σ values of 0.06, 0.08, and 0.1 where the RMSE nearly doubles—suggests a substantial degradation in performance under more challenging conditions.

σ	Resilient Controller	Baseline Controller
0.02	0.1065	0.5468
0.04	0.2209	0.8082
0.06	0.3591	1.0833
0.08	0.5002	1.3640
0.1	0.6529	1.8045

The speed profiles of the follower and leader vehicles for $\sigma=0.1$ are presented in Figure 8. This figure illustrates that the velocity of the baseline controller exhibits unacceptable behavior, characterized by rapid and sharp fluctuations throughout the simulation. Also, it experiences sudden increases, surpassing the leader's speed and potentially leading to safety hazards. In contrast, the proposed controller demonstrates a commendable performance by effectively mitigating the impacts of time delay, disturbances, and noise, therefore maintaining a safe distance from the lead vehicle.

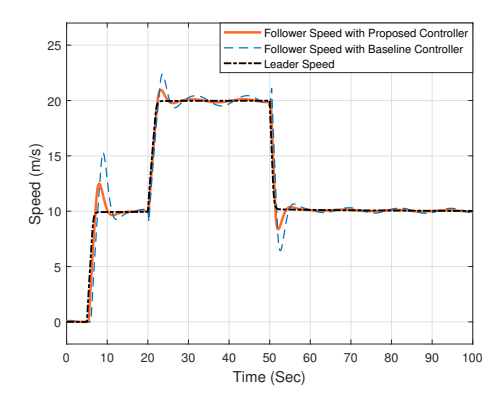


Figure 8. Speed profile for lead and follower vehicles for ($\sigma = 0.1$).

6.3. Experimental Setup Test

The real model of the Ford Fusion was utilized in both Simulink testing and experimental setup testing. The experimental setup was employed to validate the results obtained from MATLAB R2023a Simulink. This setup entailed integrating the lead vehicle and the controller within MATLAB R2023a Simulink, while a passenger vehicle—a 2017 Ford Fusion Hybrid—acted as the follower. The control signal was designed within MATLAB R2023a Simulink throughout the testing phase.

Figure 9 shows the distance between the lead and follower vehicles. As shown in the figure, our proposed controller was able to maintain a safe distance between vehicles even in the presence of a time delay in the communication channel. However, the baseline controller fails to uphold the safe distance between vehicles, resulting in an accident when the leader adjusts its velocity. In this test scenario, where the lead vehicle is virtual, negative distances were permitted while in a real-world situation, it refers to the severity of a crash. The baseline controller exhibits numerous instances of both undershooting and overshooting in vehicle distances, significantly increasing the risk of collision.

Figure 10 illustrates the velocity profiles of both lead and follower vehicles. This figure shows that the synchronization achieved by the follower with the leader's speed when utilizing the proposed controller. Conversely, under the baseline controller, at the 30-s mark, when the lead vehicle accelerates, the follower sharply increases its speed, surpassing the leader's speed and leading to a collision. This emphasizes the safe performance of the

proposed control system in adapting to dynamic scenarios and mitigating the effect of the time delay.

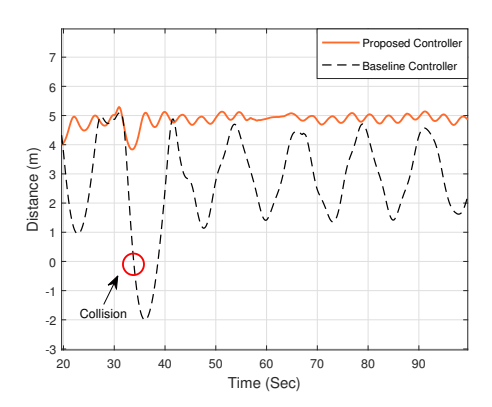


Figure 9. Distance between vehicles for $\sigma = 0.1$.

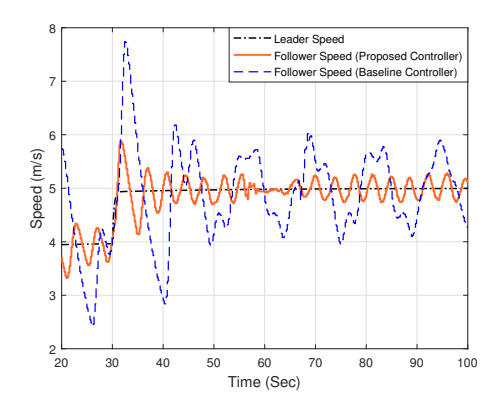


Figure 10. Speed profile for lead and follower vehicles for $\sigma = 0.1$.

7. Conclusions

7.1. Conclusions

CACC is an advanced driver-assistance system that uses communication channels to receive data from the lead vehicle. Ensuring the reliability of CACC requires safe communication between vehicles. Thus, it is imperative to identify and mitigate the negative impacts of communication delays using a safe control system. In this study, the control signal of the lead vehicle was subjected to a time-varying delay, posing significant challenges. To address these challenges, a nonlinear control system is developed to mitigate the impacts of communication delay, external disturbances, and measurement noise. The proposed design effectively mitigates the effects of time delay, disturbance, and noise, thereby ensuring a safe distance between vehicles.

7.2. Future Work

CACC might be vulnerable to cyber attacks. Therefore, additional research could focus on designing a nonlinear controller for CACC to mitigate the effects of attacks such as False-Data-Injection (FDI). Additionally, this research has centered on addressing the challenge of known time-varying time delays within the communication channel. Future investigations could be directed towards designing a safe CACC system capable of effectively mitigating the impact of unknown time-varying time delays. Moreover, this research assumes that the dynamic model of vehicles is known. Future research can focus on designing a resilient adaptive controller while the dynamic model of vehicles is only partially known.

Author Contributions: Conceptualization, P.A.B.; methodology, P.A.B.; software, P.A.B.; validation, A.S. and P.A.B.; formal analysis, P.A.B.; investigation, P.A.B.; resources, A.S. and P.A.B.; writing original draft preparation, P.A.B.; writing review and editing, A.S.; supervision, A.S.; project administration, A.S.; funding acquisition, A.S. All authors have read and agreed to the published version of the manuscript.

Funding: Partial support for this research was provided by the National Science Foundation under Grant No. ECCS-EPCN-2241718. Any opinions, findings, conclusions, or recommendations expressed in this material are those of the author(s) and do not necessarily reflect the views of the sponsoring agency.

Data Availability Statement: Data is available from the authors. Further inquiries can be directed to the corresponding author.

Conflicts of Interest: The authors declare no conflicts of interest. The funders had no role in the design of the study; in the collection, analyses, or interpretation of data; in the writing of the manuscript; or in the decision to publish the results.

Abbreviations

The following abbreviations are used in this manuscript:

CACC Cooperative Adaptive Cruise Control

ACC Adaptive Cruise Control

CAVs Connected and Autonomous Vehicles

AVs Autonomous Vehicles
CVs Connected Vehicles
V2V Vehicle to Vehicle
V2I Vehicle to Infrastructure

References

Faghihian, H.; Sargolzaei, A. Energy Efficiency of Connected Autonomous Vehicles: A Review. Electronics 2023, 12, 4086.
 [CrossRef]

- 2. Cunningham-Rush, J.; Holland, J.; Noei, S.; Sargolzaei, A. Designing and Testing A Secure Cooperative Adaptive Cruise Control under False Data Injection Attack. In Proceedings of the 2023 IEEE Conference on Dependable and Secure Computing (DSC), Tampa, FL, USA, 7–9 November 2023; pp. 1–8. [CrossRef]
- 3. Shladover, S.E. Connected and automated vehicle systems: Introduction and overview. *J. Intell. Transp. Syst.* **2018**, 22, 190–200. [CrossRef]
- 4. Guanetti, J.; Kim, Y.; Borrelli, F. Control of connected and automated vehicles: State of the art and future challenges. *Annu. Rev. Control* **2018**, 45, 18–40. [CrossRef]
- 5. Kim, M.K.; Park, J.H.; Oh, J.; Lee, W.S.; Chung, D. Identifying and prioritizing the benefits and concerns of connected and autonomous vehicles: A comparison of individual and expert perceptions. *Res. Transp. Bus. Manag.* 2019, 32, 100438. [CrossRef]
- 6. Cao, W.; Liu, S.; Li, J.; Zhang, Z.; He, H. Analysis and Design of Adaptive Cruise Control for Smart Electric Vehicle with Domain-based Poly-Service Loop Delay. *IEEE Trans. Ind. Electron.* **2022**, *70*, 866–877. [CrossRef]
- 7. Shladover, S.E.; Nowakowski, C.; Lu, X.Y.; Ferlis, R. Cooperative adaptive cruise control: Definitions and operating concepts. *Transp. Res. Rec. J. Transp. Res. Board* **2015**, 2489, 145–152. [CrossRef]
- 8. Boddupalli, S.; Rao, A.S.; Ray, S. Resilient cooperative adaptive cruise control for autonomous vehicles using machine learning. *IEEE Trans. Intell. Transp. Syst.* **2022**, 23, 15655–15672. [CrossRef]
- 9. Cui, L.; Chen, Z.; Wang, A.; Hu, J.; Park, B.B. Development of a robust cooperative adaptive cruise control with dynamic topology. *IEEE Trans. Intell. Transp. Syst.* **2021**, 23, 4279–4290. [CrossRef]
- 10. Shi, L.; Ma, Z.; Yan, S.; Ao, T. Flocking Dynamics for Cooperation-Antagonism Multi-Agent Networks Subject to Limited Communication Resources. *IEEE Trans. Circuits Syst. I Regul. Pap.* **2024**, *71*, 1396–1405. [CrossRef]
- 11. Shi, L.; Cheng, Y.; Shao, J.; Sheng, H.; Liu, Q. Cucker-Smale flocking over cooperation-competition networks. *Automatica* **2022**, 135, 109988. [CrossRef]
- 12. Shi, L.; Zheng, W.X.; Shao, J.; Cheng, Y. Sub-Super-stochastic Matrix with Applications to Bipartite Tracking Control over Signed Networks. *SIAM J. Control Optim.* **2021**, *59*, 4563–4589. [CrossRef]
- 13. Javidi Niroumand, F.; Ansari Bonab, P.; Sargolzaei, A. Security of Connected and Autonomous Vehicles: A Review of Attacks and Mitigation Strategies. In Proceedings of the SoutheastCon 2024, Atlanta, GA, USA, 15–24 March 2024.
- 14. Ploeg, J.; Scheepers, B.T.M.; van Nunen, E.; van de Wouw, N.; Nijmeijer, H. Design and experimental evaluation of cooperative adaptive cruise control. In Proceedings of the 2011 14th International IEEE Conference on Intelligent Transportation Systems (ITSC), Washington, DC, USA, 5–7 October 2011; pp. 260–265. [CrossRef]

15. Milanés, V.; Shladover, S.E.; Spring, J.; Nowakowski, C.; Kawazoe, H.; Nakamura, M. Cooperative Adaptive Cruise Control in Real Traffic Situations. *IEEE Trans. Intell. Transp. Syst.* **2014**, *15*, 296–305. [CrossRef]

- 16. Liu, Y.; Wang, W.; Hua, X.; Wang, S. Safety Analysis of a Modified Cooperative Adaptive Cruise Control Algorithm Accounting for Communication Delay. *Sustainability* **2020**, *12*, 7568. [CrossRef]
- 17. Sawant, J.; Chaskar, U.; Ginoya, D. Robust Control of Cooperative Adaptive Cruise Control in the Absence of Information About Preceding Vehicle Acceleration. *IEEE Trans. Intell. Transp. Syst.* **2021**, 22, 5589–5598. [CrossRef]
- 18. Desjardins, C.; Chaib-draa, B. Cooperative Adaptive Cruise Control: A Reinforcement Learning Approach. *IEEE Trans. Intell. Transp. Syst.* **2011**, *12*, 1248–1260. [CrossRef]
- Sargolzaei, A. A Secure Control Design for Networked Control System with Nonlinear Dynamics under False-Data-Injection Attacks. In Proceedings of the 2021 American Control Conference (ACC), New Orleans, LA, USA, 5–8 May 2021; pp. 2693–2699.
- 20. Sargolzaei, A.; Zegers, F.M.; Abbaspour, A.; Crane, C.D.; Dixon, W.E. Secure Control Design for Networked Control Systems With Nonlinear Dynamics Under Time-Delay-Switch Attacks. *IEEE Trans. Autom. Control* **2023**, *68*, 798–811. [CrossRef]
- 21. Patre, P.M.; MacKunis, W.; Kaiser, K.; Dixon, W.E. Asymptotic tracking for uncertain dynamic systems via a multilayer neural network feedforward and RISE feedback control structure. *IEEE Trans. Autom. Control* **2008**, *53*, 2180–2185. [CrossRef]
- 22. Kamalapurkar, R.; Fischer, N.; Obuz, S.; Dixon, W.E. Time-Varying Input and State Delay Compensation for Uncertain Nonlinear Systems. *IEEE Trans. Autom. Control* **2016**, *61*, 834–839. [CrossRef]

Disclaimer/Publisher's Note: The statements, opinions and data contained in all publications are solely those of the individual author(s) and contributor(s) and not of MDPI and/or the editor(s). MDPI and/or the editor(s) disclaim responsibility for any injury to people or property resulting from any ideas, methods, instructions or products referred to in the content.